PORTABLE AND MINIATURE IMAGING SYSTEM FOR IN-VIVO FLUORESCENCE /LUMINESCENCE ANALYSIS

by

ZHAOQIANG PENG

Presented to the Faculty of the Graduate School of

The University of Texas at Arlington in Partial Fulfillment

of the Requirements

for the Degree of

Masters of Science in Electrical Engineering

THE UNIVERSITY OF TEXAS AT ARLINGTON

May 2014

Acknowledgements

First and foremost, I'd like to express my sincere gratitude to my advisor Dr. Weidong Zhou for his great mentorship. He has taught me, both consciously and unconsciously, how to complete great experimental research -- strictly, smartly and speedily. I appreciate all his contributions of time, ideas and spur to make my master experience productive and stimulating. As his enthusiasm on his research was contagious and motivational for me, my positive energy is not limit to be confronted with difficulty in project, but in my life. It has been an honor to be his student.

Thanks to Dr. Liping Tang for his support and Dr. Jun Zhou, Dr. Yi-Ting Tsai for their selfless help. Their patience and immense knowledge of bioengineering and imaging processing are keys to achieve our goal. And also very thanks to another professor of my thesis committee, Dr. Yuze Sun. She has provided an excellent example as a successful woman professor.

I'm deeply grateful to Zhou Group members. They have contributed immensely to my personal and professional time at UTA. The group has been a source of friendships as well as good advice and collaboration. Thanks to these joyful people to constitute a unique harmonious working environment: Dr. Hongjun Yang, Dr. Yi-Chen Shuai, Menon Laxmy, Arvinder Singh Chadha, Shih-Chia Liu, Yonghao Liu and Nandan K Vempati. Especially, I'd like to thank Dr. Deyin Zhao who kindly taught me basic everything including the method to calibrate different physical parameters, the way to present ideas, and the approach to achieve design target.

Two years at UTA was made enjoyable in large part due to many friends that became a part of my life. I'm grateful for times spent with my friends: Shen Zhang, Yingsen Mao, Wei Xiang, Shuhong Wang, Minglu Wang, Mingmin Wang. The warm-hearted friendship is durable and memorable.

Lastly, I'd like to thanks my family for all their love and encouragement. My parents are my strong supporter in my all pursuit. And most of all for my loving, patient wife Haoze Li whose faith support during final stage of this degree is so appreciated.

04/11/2014

Abstract

PORTABLE AND MINIATURE IMAGING SYSTEM FOR IN-VIVO FLUORESCENCE /LUMINESCENCE ANALYSIS

Zhaoqiang Peng, M.S.

The University of Texas at Arlington, 2014

Supervising Professor: Weidong Zhou

For fluorescence and bioluminescence in vivo imaging system, the current commercial product is limited by huge bulk and constant working environment. In this thesis, we proposed and investigated a compact and portable in vivo device with similar performance as congeneric commercial products. By analyzing general requirements of each component in optical system, we dug in the principle and put forward to several key parameters that should be considered for building in vivo imaging system. Moreover, on the precondition of qualifying these parameters, in order to build the most compact system, three design approaches have been discussed. By deliberating each approach, the single wavelength excitation has been proposed which can be used to reduce the light path of system making it small and compact. After verifying the feasibility of single wavelength excitation, we finalized the most effective and efficient setup. Through the comprehensive calibration, we pointed out the advantage of this system and other drawbacks which can be ameliorated in future.

Table of Contents

Acknowledgements iii

Abstract v

List of Illustrations viii

Chapter 1 Introduction 1

Bioengineering Background 1

In-vivo Imaging Analysis 2

Ultrasound 2

CT X-ray 4

PET/ SPECT 5

MRI 6

Optical Methods 7

Ratiometric Approach 9

Motivation 12

Chapter 2 Requirements of System 14

Detector 14

CCD V.S. CMOS 14

Pixel Size 16

Dynamic Range 16

Signal-to-noise Ratio 17

Light Source 17

Filters 19

Colored Filter Glass 20

Thin-Film Coatings 20

Acousto-Optical Filters 21

Liquid Crystal Tunable Filters 21
Zoom-in Lens 22
Compact and Portable System Structure 23
Chapter 3 System Design 26
System I 26
System II 27
System III 29
System IV 30
Chapter 4 Single Wavelength Excitation 33
Ratio Separation 34
pH Ratiometric Analysis *In Vitro* 34
Low Concentration Detection *in Vitro* 37
Chapter 5 Real System Performance 39
Light Uniformity 39
pH Ratiometric Analysis *in Vitro* 40
Low Concentration Detection *in Vitro* 41
Low Concentration Detection *in Vivo* 44
Bioluminescence 46
Follow-up Calibration 47
Chapter 6 Conclusion 49
Appendix A Description of Components 50
Appendix B Matlab Imaging Processing Code 52
References 55
Biographical Information 58

List of Illustrations

Figure 1-1 (a) High Resolution Micro-ultrasound Machine from VisualSonics (b) Long Axis Cardiac Images from Spontaneously Hypertensive Heart Failure Rat [13] 3

Figure 1-2 (a) Micro-CT Scanner with Adaptive Geometry (b) CT X-ray Images of Side and Top Views of American Alligator from University of Utah 4

Figure 1-3 (a) Inveon PET from Siemens (b) *In vivo* PET Images of Adolescent [23] 5

Figure 1-4 (a) 9.4T Micro-MRI and Stage from Brookhaven National Laboratory (b) Areas of High Intensity Fat Depots in Mouse [24] 6

Figure 1-5 (a) Kodak In-vivo FX Pro. (b) *In vivo* Imaging of EL-4 Murine Lymphoma Tumors Implanted Subcutaneously in the Flank of Mice [25]. 7

Figure 1-6 Comparison of Several *in vivo* Imaging Technologies 8

Figure 1-7 Spectrum of Oyster680 and Oyster800 11

Figure 1-8 Emission Intensities and Ratios of pH Sensors at Different pH Values [19] 12

Figure 2-1 (a) Blue LED spectrum (b) Helium neon laser spectrum 18

Figure 2-2 Actual Transmission Curves for Two Blue-green Transmitting Colored Glass Filters [20] 20

Figure 2-3 Spectrum of the Blocked Filter [20] 21

Figure 2-4 (a) Lens with Short Focal Length (Wide Angle of View) (b) Lens with Long Focal Length (Small Picture Angle) from Nikon 22

Figure 2-5 Schematic Illustration of the Principle of Kodak In-vivo FX Pro 24

Figure 3-1 Schematic Illustration of Oblique Incident Option 27

Figure 3-2 (a) Schematic Illustration of Dichroic Mirror Option (b) 3D Structure Illumination 28

Figure 3-3 (a) Schematic Illustration of Two Wavelength Option (b) The Real Product of Two Spot LEDs Excitation 29

Figure 3-4 (a) Schematic Illustration of Single Wavelength Option (b) The Real Product of Single LED Ring Excitation 31
Figure 4-1 Spectrum of Singe Wavelength Excitation Calibration 33
Figure 4-2 Ratiometric Fluorescence: (a) Spot LEDs Two Wavelengths Excitation (b) Spot LEDs Single Wavelength Excitation 35
Figure 4-3 Ratiometric Fluorescence: (a) Kodak Two Wavelengths Excitation (b) Kodak Single Wavelength Excitation 36
Figure 4-4 Low Concentration Calibration of Single Wavelength Excitation: (a) 625nm Exciting Oyster800 (b) 735nm Exciting Oyster800 37
Figure 5-1 Light Uniformity: (a) Three Kinds of Uniformity of Light Output (b) The Cross Section of These Different Light Sources 40
Figure 5-2 Single Wavelength Ratiometric Fluorescence of LED Ring Design 41
Figure 5-3 Low Concentration Calibration: (a) 630nm LED Ring Exciting Oyster680 in BLI System (b) 630nm LED Ring Exciting Oyster800 in BLI System 42
Figure 5-4 Low Concentration Calibration: (a) 630nm Exciting Oyster680 in Kodak System (b) 630nm Exciting Oyster800 in Kodak System 43
Figure 5-5 *In vivo* Fluorescent Imaging of Concentration Calibration for Mouse 44
Figure 5-6 (a) Left: 630nm Exciting Oyster680 in LED Ring Design. Right: 630nm Exciting Oyster800 in LED Ring Design. (b) Left: 630nm Exciting Oyster680 in Kodak *In Vivo* FX Pro (saturated). Right: 630nm Exciting Oyster800 in Kodak *In Vivo* FX Pro. 45
Figure 5-7 (a) Bioluminescence Imaging by BLI System (b) *In vivo* Bioluminescence of L012 46
Figure 5-8 Definition of Working Distance 47
Figure 5-9 Calibration of Working Distance: (a) Left: 3cm. Right: 4cm. (b) Left: 5cm. Right: 6cm. 48

List of Tables

Table 1-1 Detailed Comparison of Several *in vivo* Imaging Technologies 8

Table 2-1 Detailed Comparison of Several *in vivo* Imaging Technologies 14

Table 2-2 Comparison of LED and Laser 19

Table 6-1 Specifications of BLI System 49

Chapter 1

Introduction

Bioengineering Background

In 1999, “Molecular Imaging” was proposed by Professor Ralph Weissleder and others which opened a gate to the molecular process and visualization of cellular function in living organisms without perturbing them. It also provided a better understanding of fundamental molecular pathways inside organisms [1]. To image specific molecules *in vivo*, several vital criteria must generally be met:

(a) Availability of high-affinity probes with reasonable pharmacodynamics;

(b) The ability of these probes to overcome biologic delivery barriers (vascular, interstitial, cell membrane);

(c) Use of amplification strategies (chemical or biologic);

(d) Availability of sensitive fast, high-resolution imaging techniques.

All of these four requirements should be satisfied for successful *in vivo* imaging at the molecular level.

High-affinity probes contribute on target identification and validation which is one of the key prerequisites in living systems. These probes can be small molecules, such as receptor ligands or enzyme substrates. By overcoming rapid excretion, non-specific binding, metabolism and delivery barriers, they should have the ability to reach the intended target at sufficient concentration and for a sufficient length of time to be detectable *in vivo*. To increase the imageable signal, chemical and biologic amplification strategies are developed to be used. This includes target concentration [2] and kinetics [3] improvement, avidin-biotin amplification systems [4], unique cellar functions [5], [6] and physical behavior changing [7]. After that, it’s feasible to use some “high-end” imaging technologies to detect these signals such as optical imaging technology (including diffuse

optical tomography, phase-array detection, photon counting, near-infrared fluorescence imaging). The last one is what we are working on: near-infrared fluorescence imaging with portable and compact characteristics.

In-vivo Imaging Analysis

Traditionally, *in vitro* analysis is the most common way to obtain data from tissue samples in animal. In contradistinction to traditional diagnostic imaging, the molecular imaging can detecting real time molecular abnormalities which reveals the basis of disease rather than to detect the end effect of molecular alterations. This technology sets forth to represent a novel arena for biology. Based on the theory of molecular imaging, people developed various devices utilizing different principles and mediums. These devices showed a great step from in-vitro to in-vivo noninvasive detection. Some of these devices that we can now build on include molecular cloning, micro-fabrication, chip arrays, robots, x-ray crystallography, fast mass spectrometry, and sophisticated computer analysis [1].

Generally, there are several methods to take in-vivo imaging for animals and humans that are more commonly and widely used now such as fluorescence (FLI), bioluminescence (BLI), positron emission tomography (PET), single photon emission computed tomography (SPET), magnetic resonance imaging (MRI), X-ray computed tomography(CT) and ultrasound. The obvious advantage of gaining data non-invasively and longitudinally from the same live animal are high efficiency and low waste.

Ultrasound

By the interaction of sound waves with living tissue to generate an anatomical image, ultrasound imaging allows visualization of body structures with high spatial resolution [13]. Utilizing micro-bubbles as ultrasound contrast agents is the most common way to obtain anatomical data. The gas-filled micro-bubbles are administered

intravenously to the systemic circulation and will produce a unique sonogram with increased contrast. For contrast imaging, it can reveal blood flow or drug and gene delivery.

(a)

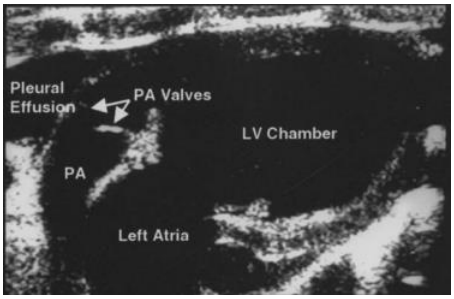

(b)

Figure 1-1 (a) High Resolution Micro-ultrasound Machine from VisualSonics (b) Long Axis Cardiac Images from Spontaneously Hypertensive Heart Failure Rat [13]

The basic components of micro-ultrasound systems include a PC, a monitor and several kinds of transducers for different applications [13]. With the simple structure and low cost, it has been widely used in pre-clinical imaging system. However, the spatial resolution is the only limitation which has been deliberated before utilizing.

CT X-ray

X-ray computed tomography (CT) is an anatomical imaging modality which presents high spatial resolution and 3D anatomical images [14]. Cone-beam x-ray source and flat panel detector with adjustable angle are most wildly used to obtain the imaging. It can finish the data acquisition in one scan to reconstruct the whole sample body [15]. The contrast of imaging depends on tissue density and contrast agents.

(a)

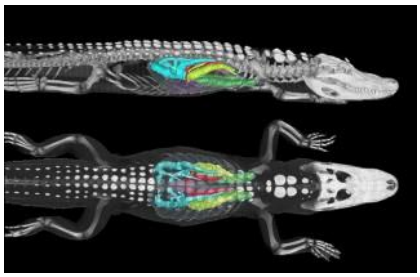

(b)

Figure 1-2 (a) Micro-CT Scanner with Adaptive Geometry (b) CT X-ray Images of Side and Top Views of American Alligator from University of Utah

Micro-CT has excellent spatial resolution especially on bone imaging. But with one of the major drawbacks of radiation dosage, it may affect the immune system as well as causing other damages. In addition, the contrast of similar tissue types is very poor which bring about limitations in research fields.

PET/ SPECT

Positron emission tomography (PET) is a clinical nuclear medicine imaging technique which produces a 3D image or picture of functional processes in the body [16]. Similar to PET, single photon emission computed tomography (SPECT) is also a nuclear medicine tomographic imaging modality commonly used in the clinic [17]. They all utilize γ-ray reacting with radioisotope that has been attached to a special ligand which relates to chemical binding properties of tissue. However, the different part locates in the γ-ray excitation and data acquisition.

(a)

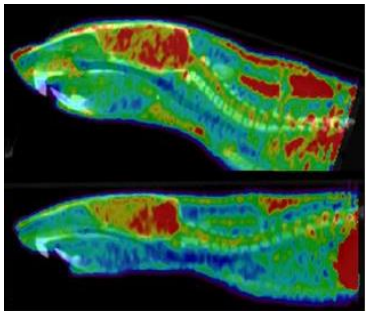

(b)

Figure 1-3 (a) Inveon PET from Siemens (b) *In vivo* PET Images of Adolescent [23]

The radiation source within the animal brings about unlimited depth of imaging. Moreover, it is very sensitive to detect similar tissue due to different radiolabelled molecular probes. However, the damage of radiation and poor spatial resolution is a major limitation.

MRI

Magnetic resonance imaging (MRI) is an anatomical imaging modality independent of ionizing radiation. MRI is suitable to longitudinal studies because it is non-invasive [18]. The excellence in accuracy of 3D imaging can provide anatomic organ and pathology definition by high spatial resolution which can also be improved by better signal-to-noise ratios. MRI has the advantage at morphological imaging and functional imaging.

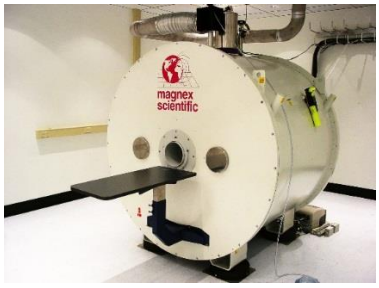

(a)

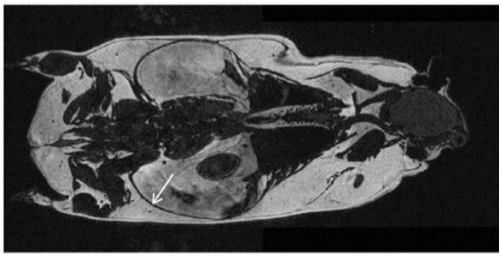

(b)

Figure 1-4 (a) 9.4T Micro-MRI and Stage from Brookhaven National Laboratory (b) Areas of High Intensity Fat Depots in Mouse [24]

The advantage of micro-MRI is the perfect spatial resolution and excellent contrast. But with complex construct, the cost of MRI devices is extremely expensive.

Optical Methods

Animal models of disease can be monitored by means of fluorescence (FLI) or bioluminescence (BLI) reporters [8]. For bioluminescence, it is a kind of cold body radiation outputted from a substrate by using luciferase to label cells and gene which can bring out the production and emission of light from a living organism. For fluorescence, it is similar to luminescence but the emission of light by a substance labeling with fluorescent reporters such as GFP, RFP, Cyt and dyes [9] that have absorbed light or other electromagnetic radiation. Usually it will emit a longer wavelength than the absorbed radiation.

(a)

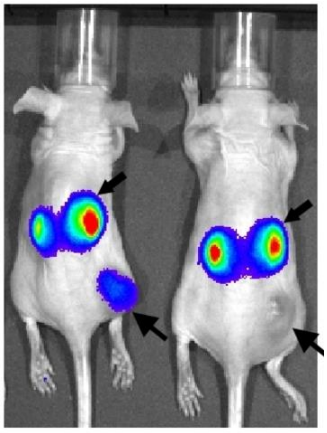

(b)

Figure 1-5 (a) Kodak In-vivo FX Pro. (b) *In vivo* Imaging of EL-4 Murine Lymphoma Tumors Implanted Subcutaneously in the Flank of Mice [25].

In vivo optical imaging in animals and the human body is popular in preclinical drug discovery and can evaluate drug efficacy, pharmacodynamics [10], pharmacokinetics and bio-distribution through labeling with light sensitive reporters. The emitting light from the body is detected by a high sensitivity cooled charged-coupled device camera [11]. And the imaging processing allows for real time 2D or 3D reconstruction. The longitudinal, quantitative, non-invasive characters helps to analyze tumor cells or infectious disease by labeling with a constitutively expressed protein [12].

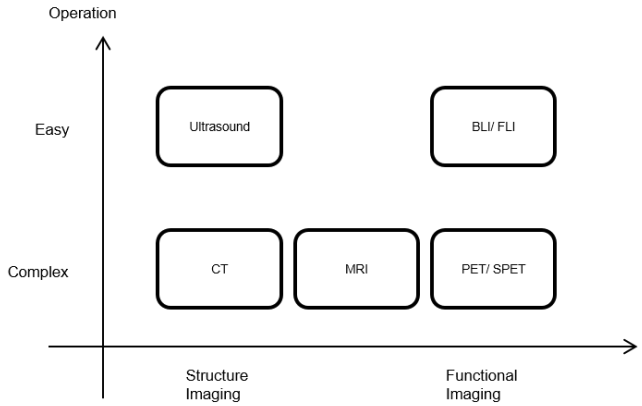

Figure 1-6 Comparison of Several *in vivo* Imaging Technologies

Optical methods are fastest and easy to use for pre-clinical imaging detection. It is also inexpensive and sensitive depending on the property of CCD. Although the major weakness is depth of penetration which is limited by visible dyes of a few millimeters, near-infrared fluorescence allows access to several centimeters to detect the emission light.

Table 1-1 Detailed Comparison of Several *in vivo* Imaging Technologies

Imaging Modalities	Applications	Advantages	Disadvantages
Fluorescence(FLI)	reporter gene expression; cell, virus, bacteria, protein, small molecule tracking	high sensitivity; easy operation; low-cost; high throughput	low spatial resolution; low specificity; poisonous fluorescent dyes

Table 1.1—*Continued*

Bioluminescence(BLI)	reporter gene expression; cell, virus, bacteria tracking	high sensitivity; fast; easy operation; low-cost; high throughput	low spatial resolution; 2-D imaging
Positron emission tomography (PET)	reporter gene expression; small molecule tracking	high sensitivity; quantitative analysis	low spatial resolution; radiation damage; expensive
Single photon emission computed tomography (SPET)	reporter gene expression; small molecule tracking	clinical imaging	low spatial resolution; radiation damage; expensive
Magnetic resonance imaging (MRI)	morphology	high spatial resolution	low sensitivity; long operation time; expensive
X-ray computed tomography(CT)	oncology; osteopathic medicine	anatomical imaging	limited applications; radiation damage
Ultrasound	cardiovascular; neurosciences	real time imaging; low-cost	limited spatial resolution

Ratiometric Approach

Fluorescence imaging and bioluminescence imaging are widely used on pharmacodynamics, pharmacokinetics and bio-distribution by tracking cell, virus, bacteria, protein, and small molecule. By labelling with a constitutively expressed protein, the longitudinal, quantitative, non-invasive characters helps to analyze tumor cells or inflammatory reactions by measurement of intracellular pH value.

Intracellular pH plays many vital roles in cell, enzyme, and tissue activities, including proliferation and apoptosis, multidrug resistance (MDR), ion transport, endocytosis, and muscle contraction. Monitoring pH changes inside living cells is also significant for studying cellular internalization pathways, such as phagocytosis, endocytosis, and receptor ligand internalization. Changes of pH affect the nervous system as well, by influencing synaptic transmission, neuronal excitability, cell-cell coupling via gap junctions, and signal cascades. Abnormal pH values are associated with

inappropriate cell function, growth, and division and are observed in some common disease types such as cancer and Alzheimer's. [3]

Intimate connections between the cell functions with intracellular pH means that precise measurement of intracellular pH can provide critical information for studying physiological and pathological processes down to a single organelle. Good resolution in the space and time dimensions, i.e., spatial and temporal, is highly desirable. Compared to other pH measurement methods such as microelectrodes, NMR, and absorbance spectroscopy, fluorescence spectroscopy has advantages with respect to spatial and temporal observation of pH changes. Moreover, fluorescence techniques have high sensitivities, they tend to be operationally simple, and they are in most cases nondestructive to cells [4]. Qualitative measurements of pH can be achieved using fluorescent indicators that switch on or off at sharply defined pH values. However, such measurements may be influenced by many factors, including optical path length, changes of temperature, altered excitation intensities, and varied emission collection efficiencies. The alternative is to use "ratiometric detection". Ratiometric spectroscopic methods require fluorescent sensors that are differentially sensitive to the analyte (i.e., protons for pH probes) for at least two excitation or emission wavelengths (Figure1.7). For instance, for a suitable fluorescent dye, emission at one carefully chosen wavelength may be enhanced or diminished relative to the emission at another. Ratios between these signals can then be calibrated to indicate pH values. Advantages when using ratiometric methods are accrued because parameters such as optical path length, local probe concentration, photo bleaching, and leakage from the cells are irrelevant. This must be so since both signals come from the probe in exactly the same environment. [2]

Since the traditional preparation and analysis of tissue sample is time-consuming, the optical method brings about innovation in this area. The dynamic

response accompanied by specific pH changes are difficult to continuously monitor and evaluate the inflammatory response *in vivo*. A new ratiometric optical pH probe which combines pH-sensitive (CypHer5E/Oyster680) and pH-insensitive (Oyster800) fluorescent dyes together is developed to solve this problem [19]. CypHer5E or Oyster680 are pH-sensitive cyanine dye since their fluorescent emissions depend on pH value. Generally, they can be used alternatively due to the similar spectrum. At neutral pH, they perform minimal fluorescence but become highly as an emission peak at 670nm in an acidic environment. On the other hand, Oyster800 has a constant fluorescence with an emission peak at about 794 nm regardless of pH value. These two dyes are conjugated together to fabricate pH sensors on the surface of PNIAPM spheres.

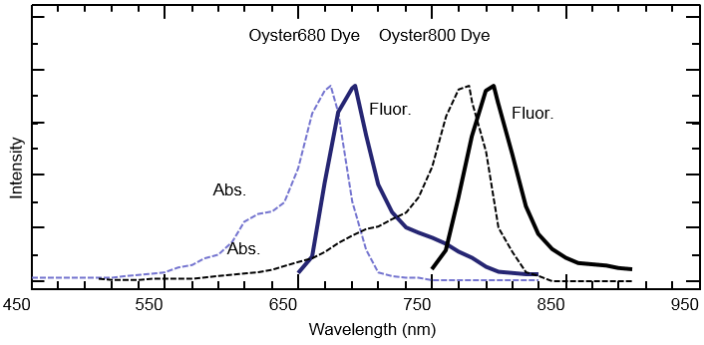

Figure 1-7 Spectrum of Oyster680 and Oyster800

The emission light from these two dyes in nanoparticles for *in vivo* imaging can generate more accurate information by taking the ratio of fluorescence intensities at different wavelengths. These nano-sized sensors provide excellent measurement capabilities for three different inflammation models. There is a strong positive correlation found between ratiometric pH changes and the inflammatory response. Hence, utilizing this effective method, we can get a noninvasive, rapid and highly sensitive optical readout for pH-ratio changes *in vivo*.

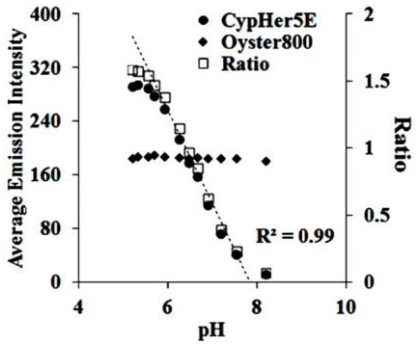

Figure 1-8 Emission Intensities and Ratios of pH Sensors at Different pH Values [19]

By increasing the pH value, the average fluorescence intensities from CypHer5E/Oyster680 were substantially decreased, whereas the average fluorescence intensities from Oyster800 were unchanged throughout the pH range. The ratios of the average fluorescence intensities between CypHer5E/Oyster680 (pH-sensitive dyes, with average intensities of fluorescence from 630–730 nm) and Oyster800 (pH-insensitive dye, with average intensities of fluorescence from 800–860 nm) were also calculated to provide quantitative measurement of the pH in an aqueous environment [19].

Motivation

Researchers have designed several kinds of optical devices to process *in vivo* imaging analysis in the laboratory. While these benchtop devices have produced reliable and repeatable data from small objects, as well as from anesthetized mouse with implanted tumor cells, such devices are large and cumbersome and further require the individual small animal to be placed within a full body enclosure. Other advanced applications, such as human subject research, may require that the device is capable on small scale free space detection without a full body enclosure and that it is portable to carry on. In fact, a laboratory is not a beneficial place for fast clinical diagnosis by using large bulky device. Thus, some of the current devices are less than ideal for routine clinical practice and investigations.

A near-infrared (NIR)-based, non-invasive, portable imager was designed by us which circumvented the above problems with minimal complexity. The long-term goal of the project is to bring to the market a new tool for fluorescence and bioluminescence detection which aids on clinical research and provides real time 2-D imaging of fluorescence or long exposure time bioluminescence. In addition, an easily carried and light weight device allows researchers to manipulate it in multi-culture environment with immense application without being limited in laboratory. As a compact and portable device, it is totally feasible to be built like an external attachment with all components integrated as an entity to mount on a camera. With this mount-and-play device, *in vivo* clinical diagnosis is able to be pushed forward to be a fast, efficient, and friendly operation.

Chapter 2

Requirements of System

Due to the high efficiency of optical approach and principle of monitoring *in vivo* inflammatory responses using a pH ratiometric fluorescence imaging probe, we proposed an *in vivo* imaging system with advantages of compact and portable. In this section, requirements of each component in optical system has been discussed.

Table 2-1 Detailed Comparison of Several *in vivo* Imaging Technologies

Detector	Sensors	CCD
	Pixel Size	5 ~ 10μm
	Dynamic Range	16 bit
	Dark Current	< 0.001 electrons/pixel/s
	Read Noise	< 100 electrons (rms)
Light Source	Sensors	LED
	Wavelengths	Around 674nm or 778nm
Filter	Type	Thin-film Coatings
	Transmission	>60%
Zoom Lens	Angle of View	>28°

Detector

Based on the principle of fluorescence and bioluminescence, the low intensity of emission light from biosensor is a problem for the system to obtain the data with high clarity. For continuous studies, high quality imaging play a vital role in biology analysis. Hence, selecting the most suitable detector is necessary to be considered.

CCD V.S. CMOS

Two main technologies on capturing image digitally most widely used are CCD (charge coupled device) and CMOS (complementary metal oxide semiconductor). The unique advantages and disadvantages of each one have been applied in different research area. By analyzing these characteristics, it’s obvious to find the most appropriate detector for near-infrared *in vivo* imaging system.

Although these two kinds of imager sensors have the same function of converting the light into electric charge as electronic signals, these are innate differences in their structure. In a CCD sensor, a limited number of output nodes control every pixel's charge into voltage as an analog signal. These pixels contribute on light capture with a high uniformity of output. On the contrary, in CMOS sensor, each pixel has its own charge-to-voltage conversion, amplifiers, noise-correction, and digitization circuits. These functions increase the complexity of design and reduce the available area for image capture. Although it allows high light capture with wide bandwidth for high speed, since each pixel is working individually, the uniformity of detection is low.

For near infrared light detection which requires a thicker photon absorption region since infrared photons are absorbed deeper than visible photons in silicon, CMOS sensors can't achieve enough sensitivity in this spectrum region. Increasing the thickness of substrate to enhance the infrared sensitivity will bring about a decrease in the ability to resolve spatial features. But for CCD sensors, comparing with nearly 10 microns thick of substrate in CMOS, it can achieve 100 microns thick which can be used as highly sensitive in the near infrared.

Since the fluorescence requires high uniform and near-infrared imaging detection, the charge-coupled device (CCD) camera is the most appropriate component in the system. In fact, the development of bioluminescence and fluorescence imager mainly depends on the invention of cooled back-illuminated CCD camera. Due to the research of high quantum efficiency CCD, in-vivo imaging has become more and more sensitive which becomes capable on pre-clinic research such as in small metastases tumor detection.

There are several CCD properties to influence system performance. By analyzing these properties, we can find several key specifications which should meet evaluation standards.

Pixel Size

Increasing the size of pixel can bring about the improvement of sensitivity. More electronics can be collected by single pixel which is able to generate more signals. Moreover, higher binning value also make bigger photon sensitive area which is capable to detect weak signals. However, big pixel size means low resolution resulting in output image with low clarity. On the contrary, small pixel size can lead to high level resolution but low sensitivity, low signal-to-noise ratio and low dynamic range.

Hence, in order to obtain better quality imaging, it's necessary to keep a balance between the choice of cameras with big size pixel or small size. Normally in the commercial market, for high sensitivity CCD camera, the pixel size is around 5μm to 10μm which is capable on near-infrared imaging detection.

Dynamic Range

To describe dynamic range we use the term data bit value which indicates the gray scale of output image. If scale is 16 bit, the data contained in image detecting by each pixel has $0\sim2^{16}$ values to represent signal strength. The camera with high dynamic range is capable on fluorescence and bioluminescent research which required the ability to distinguish slight difference of signals.

Therefore, in order to process more precise analysis, the dynamic range of *in vivo* imaging systems should be 16 bit which is also the main type of the commercial product.

Signal-to-noise Ratio

For same level CCD chips, signal-to-noise ratio (SNR) is significant to the quality of output image. SNR is not only related to innate property of CCD and also bound up to the whole setup of system and environment.

$$SNR = \frac{I * QE * t}{\sqrt{(I * QE * t + Nd * t + Nr^2)}}$$

Where I is the incident photon flux (photons/pixel/second), QE represents the CCD quantum efficiency, t is the integration time (seconds), Nd is the dark current value (electrons/pixel/second), and Nr represents read noise (electrons). As the equation shows the calculation of SNR, it's obviously to find the key parameters to effect SNR are quantum efficiency, dark noise and read noise.

There is an intimate connection between dark noise and temperature. In the general case, lower temperature informs less dark noise being generated. But when the temperature goes down to a certain level, spurious charge will increase the dark noise. Hence, there should be an optimum value for temperature. In addition, the dark current and read noise should be as small as possible such as smaller than 0.001 electrons/pixel/s and 100 electrons (rms).

Light Source

There are three kinds of light source which qualify the requirement of fluorescence: light-emitting diode (LED), laser, and gas-discharge lamp. By the unique characteristic of each technology, they have different application in different research field. Under these technologies, there are many branches which have been developed: LED ring, LED spot light, fiber-coupled laser source, and fiber optic illuminator.

LEDs are based on p-n junction which can release photons whereas electronics recombine with holes. Laser consists of a gain medium, a pumping source, and mirrors

which can amplify light by stimulating emission. Gas-discharge lamps are utilized to generate light by sending and electrical discharge through an ionized gas or plasma which can be controlled by pressure of the gas as well as the frequency of the current.

First of all, due to the requirement of fluorescence imaging, the bandwidth of excitation light should be narrow in order to avoid exciting adjacent dyes. Since the excitation spectrum of Oyster680 is around 674nm and Oyster800 is around 778nm, it's obviously to find that bandwidth should be no more than 50nm. Also, the light should be collimated to form a perfect uniformity, which is achieved by collimator and excitation filters but conflicts with compact size. In this way, gas-discharge lamps don't qualify for the basic requirements of the compact system since its huge size and wide bandwidth of non-monochrome.

Second, besides gas-discharge lamps, LEDs and laser are more appropriate to build a compact device.

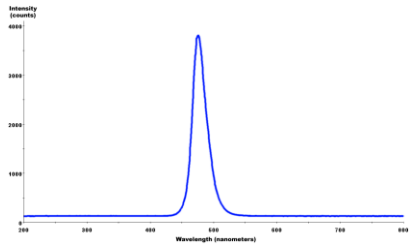

(a)

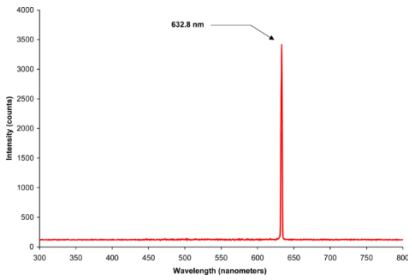

(b)

Figure 2-1 (a) Blue LED spectrum (b) Helium neon laser spectrum

Depending on the fundamental principle of laser and LEDs, it's obviously to find that the structure in laser is much more complex than LEDs. By this complex structure, the light emitted from laser is coherent and monochrome but with a small beam size. On the contrary, for LEDs, the emission light is incoherent, with big beam size, and the bandwidth can't be very narrow. Since laser can't achieve enough beam size without complex setup, LEDs are the most appropriate choice.

Table 2-2 Comparison of LED and Laser

Parameter	LED	LASER
Wavelength Content	Large	Small (desirable; more monochromatic)
Spectral Width/Line Width	50 nm	< 5 nm
Principle of Emission	Spontaneous; random photon emission (hence, not directional)	Stimulated
Coherence	Incoherent; since emission is spontaneous	Coherent; since emission is stimulated; same phase as the stimulating photon
Output Power	Low	High
Directionality	Low	Highly directional
Speed of Operation	Slow	Faster
Ease of Use	Easier to use; less complex circuitry	Complex circuitry; thermal & optical stabilization circuits
Lifetime	Long	Shorter
Cost	Cheaper	Expensive

Filters

There are two main types of filter technology most widely used in fluorescence analysis: colored filter glass and thin-film coatings. Besides, utilizing acousto-optical tunable filters in special applications is widespread. Others such as holographic filters and liquid crystal tunable filters are also beneficial in some areas but not for fluorescence. To build the fluorescence and bioluminescence system, the filter is required as high peak transmittance and sharp slope which should be thin-film coatings.

Colored Filter Glass

Another name of colored filter glass is absorption glass which is the most widely used type of filter in fluorescence analysis. The ability of filter glass to attenuate the light depends on the physical thickness of glass since the only physical phenomenon is absorption. Therefore, if increasing the thickness, blocking level will increase, but also reducing peak in band transmission which means there should be an optimum thickness value.

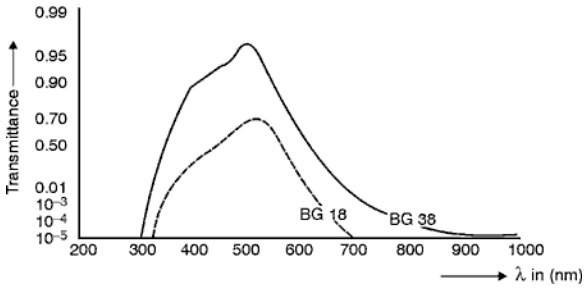

Figure 2-2 Actual Transmission Curves for Two Blue-green Transmitting Colored Glass Filters [20]

The colored filter glass is inexpensive and stable for normal conditions, and the characteristic of spectrum is independent of incident angle. However, there are several disadvantages: limited glasses selection, poor slope and low peak transmittance [20]. From figure 2-2, it's obviously to find that the slope is very poor and the thickness factor also affects the performance of color filter glass.

Thin-Film Coatings

Two kinds of thin-film coatings are often used: metallic coatings for total reflective mirrors and neutral density filters; thin-film interference coatings. The later one is the main component of interference filter. A stack of thin layers of material form the overlap of reflection and transmission which has a huge flexibility of performance [20].

By adjusting the number of layers and the selection of material, it's feasible to achieve bandpass, shortpass and longpass filters with good performance. However, interference coatings are highly sensitive to incident angle. As the angle varies, the spectrum may generate red shift or blue shift.

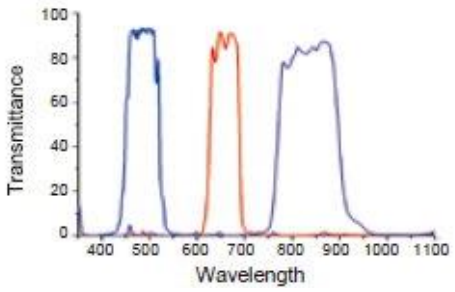

Figure 2-3 Spectrum of the Blocked Filter [20]

From figure 2-3, by comparing with color glass filters, it's obviously to find the sharp slope and narrow bandwidth as characteristics of thin-film coating filters is the most suitable type of filter can be used on fluorescent detection.

Acousto-Optical Filters

The acousto-optical tunable filter (AOTF) is increasingly used as excitation filters. By setting up radio-frequency acoustical vibrations in crystal performs similar as diffraction grating [21].

Varying the frequency effects the period of grating which control the wavelength of diffractive light. The maximum accepted incident angle can be 5 degrees. And since it's electronically controlled device, the system can be automatic operation. However, the full width at half maximum (FWHM) is limited such as 2 nm in the visible. The physical dimension such as aperture and thickness is limited.

Liquid Crystal Tunable Filters

The liquid crystal tunable filter (LCTF) is increasing used as emission filters. In the center of LCTF, a series of waveplates consisted of a layer of birefringent material

paired with a liquid crystal layer inducing wavelength-dependent rotation of the incident polarized light. The magnitude of the waveplate is controllable by voltage applied to transparent conductive coatings. LCTF can achieve variable attenuation capabilities and controllable bandwidths (FWHM).

Zoom-in Lens

The curvature of two optical surfaces determines the type of lens. Each surfaces can be convex or concave to form different lenses with different optical properties. The most typical lenses are biconvex and biconcave. These two are widely used in many field of optical systems. By assembling several lens elements to build a zoom lens, it is able to vary in focal length and angle of view.

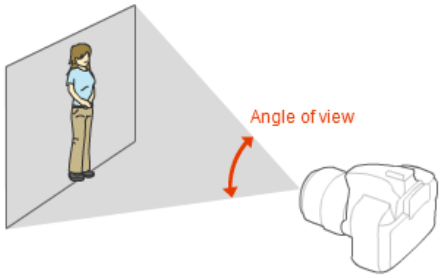

(a)

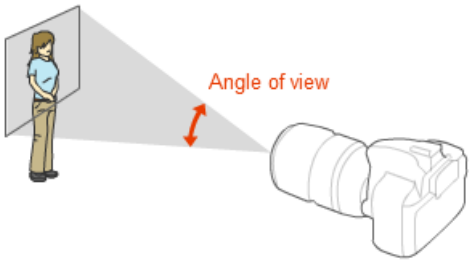

(b)

Figure 2-4 (a) Lens with Short Focal Length (Wide Angle of View) (b) Lens with Long Focal Length (Small Picture Angle) from Nikon

The focal length of an optical system is defined as the distance of converging light. In fact, in most applications, long focal length leads to higher magnification and narrow angle of view if the subject is essentially infinitely far away. Contrarily, short focal length means wide angle of view. The angle of view, which is same as field of view, is defined as the angular extent of a given scene. It is not the same as angle of coverage which describes the angle range that a lens can image. Generally, the visible extent of the scene captured by the image sensor is angle of view which is stated as an angle. Wide angle of views capture greater areas, small angles capture smaller areas. If the object is close enough to the lens, a shorter focal length results in high magnification and wild angle of view.

$$\alpha = 2\arctan(\frac{h}{2f})$$

At infinity focus, f=focal length and h=image size. Therefore, if the working distance of compact fluorescent system is less than 10cm which supposed to be focal length, and the detection area should be more than 2.5cm^2, we can calculate the angle of view is 28°. That means the requirement of angle of field for zoom lens should be more than 28° vertically or horizontally.

Since there is no perfect lens, different loss can be made to achieve different properties. It's a compromise of focal length range, image quality, aberrations, and other features. For compact fluorescent imaging system, the basic requirement of zoom lens is on the angle of view. The angle of view should be enough to cover enough detection area.

Compact and Portable System Structure

The need to have high quality imager embedded in the smallest of devices is increasing by the day. People realize huge potential underlying this technology and realize

a compact and portable imager would enable people in many ways such as real-time noninvasive monitoring of in-vivo and in-vitro research.

Bioluminescence & fluorescence imager with optical module helped to analyze *in vivo* imaging, such as ratiometric fluorescence, and is a mature technology in the current commercial market. Figure 2.5 shows the structure of Kodak *in vivo* FX Pro. *In vivo* imaging system is constructed with two parts: excitation and emission. The excitation usually includes light source, collimator and monochrome module. In emission, the detector and filter are most adopted. Each component plays a significant role in the entire system. Normally, it is designed as large bulky light-tight chamber with electronically controllable components. After the white light filters by excitation to form the selection of wavelengths, the biosensor is able to absorb that specific wavelength and emit the longer wavelength. Passing through emission filters, CCD camera can collect the signal.

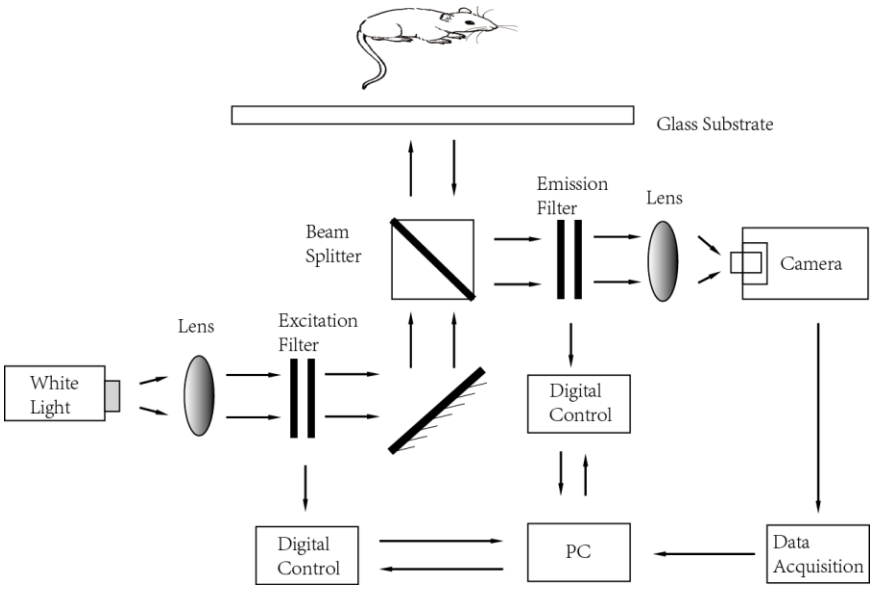

Figure 2-5 Schematic Illustration of the Principle of Kodak In-vivo FX Pro

As figure 2-5 shows the light path in Kodak In-vivo FX Pro system, it's obvious to notice the excitation filter, emission filter, beam splitter and glass substrate are

characteristics of the whole system which construct a large device. The white light generated by 175W xenon LED passes through excitation filter to become the specific wavelength. Then it reflected by mirror and goes through beam splitter straight to arrive at the sample. The emission light from samples passing the glass substrate and reflecting by beam splitter, going through emission filter, finally arrive at the camera. In the Kodak system, there are bountiful choices of excitation filters and emission filters because of large space.

Reducing the complex light path is a method to make the device miniature. By ensuring the key component in the system which is capable of fluorescent detection, the quality of the image can be ameliorated by imaging processing. However, the design of the Kodak system is not suitable for compact and portable target since it has a huge light filtering system. By reducing the size, there is a way to consider monochrome light source such as LED and laser. Since the intensity of the laser beam is too strong, it may produce damage to the animal whereas too small beam size, LED is another good choice.

Chapter 3

System Design

In this section, I'll demonstrate envisaging of the desirable system including customized components. Some of them are not suitable due to strong background noise and bad light uniformity. However, by thinking of these ideas, it's obviously to constitute the rational product.

First of all, due to the principle analysis above, key components are indispensable. To ameliorate system performance, how to go about designing a light path becomes a problem. Considering the requirement of the system, several thoughts come to mind.

System I

In order to minimize the effect of detecting the light from the light source, the simplest method is utilizing oblique incidence and detection to separate the system into two parts: excitation and emission. The monochrome light filtered by thin-film coating filters is absorbed by biosensors in sample and signaling of the fluorescent light detected by CCD camera. In addition, by adding a box to cover the whole system, it is able to reduce ambient background noise.

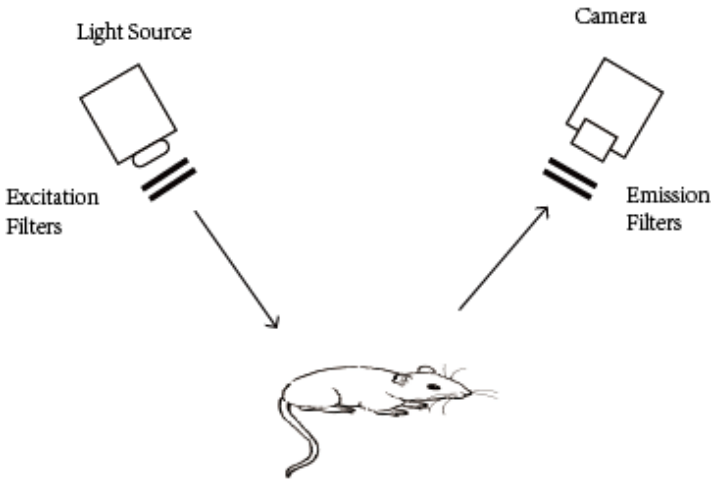

Figure 3-1 Schematic Illustration of Oblique Incident Option

However, this design is not an excellent option for a compact and portable system. Considering the large size to arrange the light path in this design and filtering light in free space, we suspend it to instead design a system without too many complex components.

System II

If combining LED with a dichroic mirror, we can build a compact optical module. It avoids free space in light path and recognizes the compact design. Dichroic mirrors (or beam splitters) are able to guide the light by selectively transmitting and reflecting different wavelengths. Generally, it is most widely used on multiple LEDs into a common light path, or splitting white light or fluorescence excitation and emission bands into discrete components. In fact, the array of LEDs can achieve high uniformity and multi-wavelength by arranging different kinds of LEDs. In addition, the property of dichroic mirror reflecting a specific wavelength and transmitting others is helpful for single wavelength excitation. Using short wavelength is able to excite high energy level which is approved by the principle above.

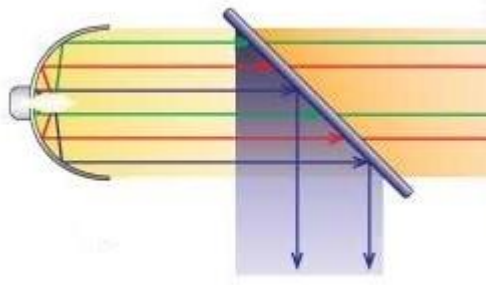

(a)

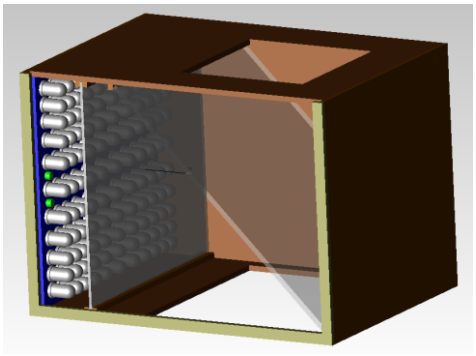

(b)

Figure 3-2 (a) Schematic Illustration of Dichroic Mirror Option (b) 3D Structure Illumination

The light of LEDs reflected by dichroic mirror downward to samples with single wavelength due to its bandwidth. The biosensor in the sample absorbs the excitation light and emits the emission light with longer wavelength. If this longer wavelength exceeds the bandwidth of dichroic mirror, it will pass through and upwards to CCD without any blocking.

However, it's can't improve the field of view by zoom-lens since the size of dichroic mirror limit the aperture. Another issue is that dichroic mirror can only reflect narrow bandwidth light from LEDs and it may be impossible to implement two

wavelengths excitation. Hence the feasibility of a single wavelength excitation needs to be verified.

System III

To balance the un-stable properties in oblique incidence and detection, and complex structure in dichroic mirror, we put forward a design of two LEDs with spot light emitting two wavelengths (figure 3-3). It has benefits such as zoom-in lens which can control field of view, two monochrome spot LEDs which don't need excitation filter, and oblique incidence and vertical detection to minimize the light path.

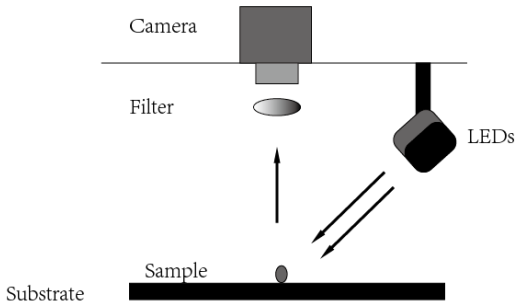

(a)

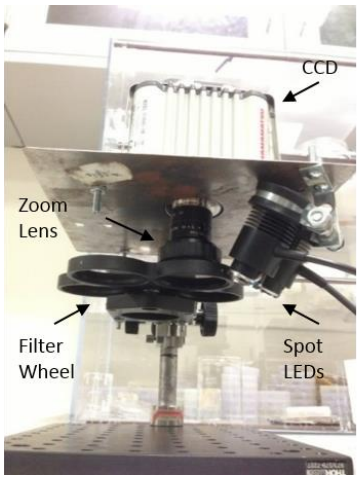

(b)

Figure 3-3 (a) Schematic Illustration of Two Wavelength Option (b) The Real Product of Two Spot LEDs Excitation

The light emitted from two monochrome spot lights don't need excitation filter to narrow the bandwidth which reduce the system size. By absorbing the excitation light, biosensors emit longer wavelength to all sides. Vertically, the emission light passed through filter wheel enters the zoom lens, and is then collected by CCD camera. The emission filter wheel allows multiple choices to select the wavelength of detection. This system is built on the fundamentals of ratiometric fluorescence pH probe since it needs two dyes to complete the research, which corresponds to two monochrome spot LEDs.

System IV

In order to compensate the limit of flaws in two wavelengths construct, and to verify the feasibility of single wavelength excitation, adopting LED ring is a good choice. LED ring is a kind of array of LEDs as a ring with LEDs at the edge and empty at the center. It can make the system totally vertical, since the light emits from edge downwards to samples, then the emission light passes through the center of the LED ring being collected by CCD camera. Due to the divergence angle of LEDs, LED ring can achieve uniform light by arranging LED on an appropriate array and working on a suitable distance. However, it limits the selection of lights with different wavelengths. Stagger arrangement of LEDs is the way to achieve wavelengths selections while reducing the uniformity. To compensate this flaw, we have built the device based on single wavelength excitation.

Since single wavelength is theoretically enough to excite two dyes, LED ring can perform uniform light and avoid blocking the emission light through camera. In addition, it's easy to mount on the zoom-in lens since it is a small entity. However, the feasibility of single wavelength exciting two dyes needs to be verified, which is discussed in the next section. Based on Oyster800 spectrum, the peak of excitation intensity locates on 778nm, and the peak of excitation intensity for Oyster680 locates on 674nm. In the

spectrum, there is some overlapping in the absorption region of two dyes but with low quantum efficiency. If we only use 630nm wavelength light to excite two dyes, it brings about the emission lights of Oyster680 and is much stronger than Oyster800 which mainly relied on emission filter to receive the true signal.

Due to the properties of LED ring and thin-film coating filters, it's possible to reduce the device size. The light emitted by LED ring enters the biosensor in the samples (figure 3-4), then passes through LED ring received by CCD camera under the perfect performance, such as uniform light and sensitive detection.

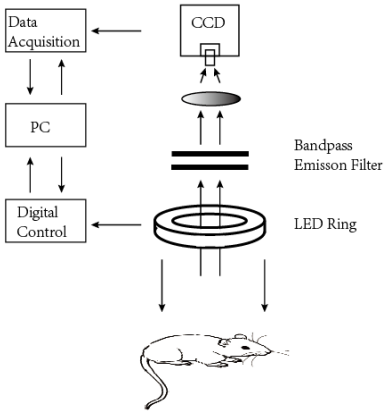

(a)

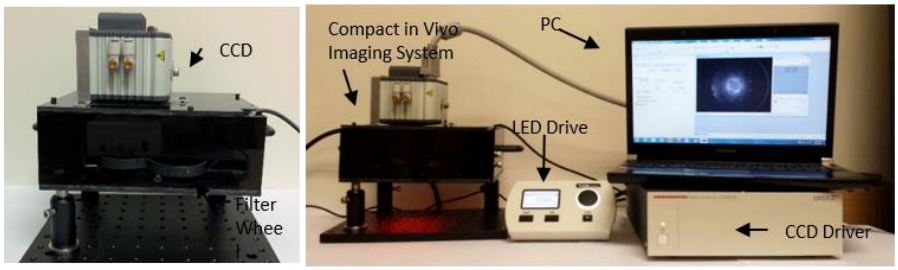

(b)

Figure 3-4 (a) Schematic Illustration of Single Wavelength Option (b) The Real Product of Single LED Ring Excitation

The system is covered by a plastic box which can block the ambient light most efficiently. By cutting a window on the side of the box, manually controlled filter wheel allow to change the emission filters without disturbing the measurement process. Moreover, the electronically controlled LED ring also allows changing the intensity of the excitation light through PC software.

Chapter 4

Single Wavelength Excitation

In theory, the peak wavelength of excitation for Oyster680 and Oyster800 are different. One locates at 674nm whereas another one at 778nm. That means if wavelength of excitation lights around that specific value, the quantum efficiency will be stronger. However, due to the principle of quantum properties, if there is an overlapping region of excitation wavelength in spectrum for Oyster680 and Oyster800, 625nm is enough to excite two different dyes. Therefore, two different methods need to be compared.

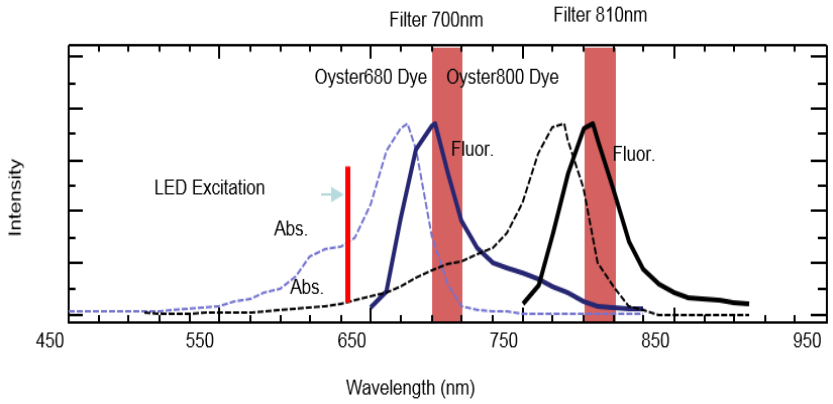

Figure 4-1 Spectrum of Singe Wavelength Excitation Calibration

In figure 4-1, the absorption spectrum of two dyes are covered around 625nm which brings about the feasibility one wavelength exciting Oyster680 and Oyster800 at same time. Theoretically, when the emission bandpass filter is 700nm, we can receive the signal only from Oyster680, but the signal from both Oyster680 and Oyster800 when changing to bandpass filter is 810nm. It's obviously to be found in the spectrum which has two fluorescence spectrums around 810nm. To separate this overlap and reveal the real signal from Oyster800, we proposed an imaging processing method.

Ratio Separation

Oyster680 is a pH sensitive dye whereas Oyster800 is in-sensitive. There must be a correlation between the emission from Oyster680 and pH value but not for Oyster800. Therefore, since we use 700nm bandpass filter, and the signal from Oyster680, we can conclude an equation:

$$I_{700} = pH \times QE_{11} \times I_{in}$$

QE presents quantum efficiency. I_{in} is excitation intensity. And I_{700} presents the signal collected when using 700nm bandpass filter. On the other hand, when changing to 810nm bandpass filter, we can conclude an equation:

$$I_{800} = pH \times QE_{12} \times I_{in} + QE_{2} \times I_{in}$$

The signal collected when using 810nm bandpass filter contains two parts which are signals from two dyes. The former part is pH sensitive which from is Oyster680, whereas the later pH insensitive part is from Oyster800. After that, we supposed a new factor R which equals to QE_{12}/QE_{11}. Hence, the equation can be changed to:

$$I_{810} = R \times I_{700} + QE_{2} \times I_{in}$$

Two measurable quantities I_{700} and I_{810} can result in the R value by analyzing the linear fitting of data. Based on the R value, we can derivate an equation of fluorescence from Oyster800 when using 810nm bandpass filter:

$$Fluo_{Oyster800} = I_{810} - R \times I_{700}$$

This imaging processing method compensates the flaw of single wavelength excitation that separates the signal from Oyster680 and Oyster800 when using bandpass filter 810nm. According to this, we can result in an acceptable ratiometric measurement.

pH Ratiometric Analysis *In Vitro*

By taking the ratio of 625nm exciting Oyster680 over 735nm exciting Oyster800 comparing with the ratio of 625nm exciting Oyster680 over 625nm exciting Oyster800, we

can see the feasibility of single wavelength excitation for pH ratiometric fluorescent imaging.

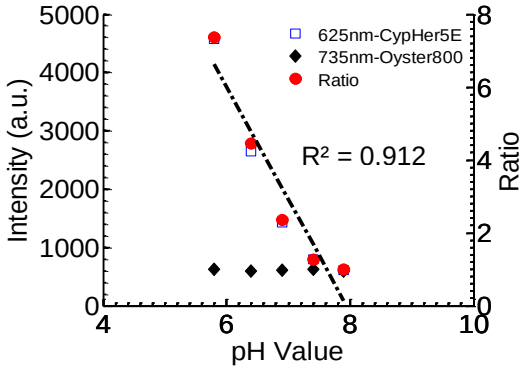

(a)

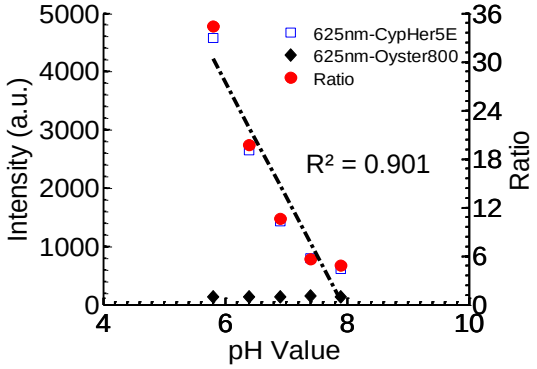

(b)

Figure 4-2 Ratiometric Fluorescence: (a) Spot LEDs Two Wavelengths Excitation (b) Spot LEDs Single Wavelength Excitation

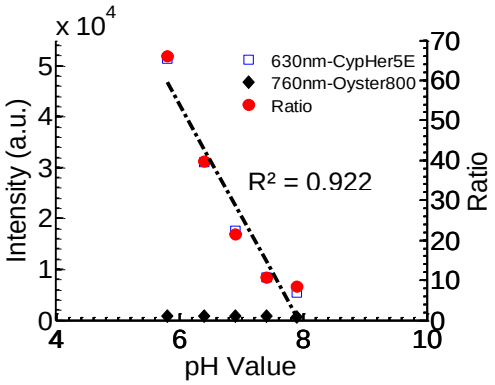

(a)

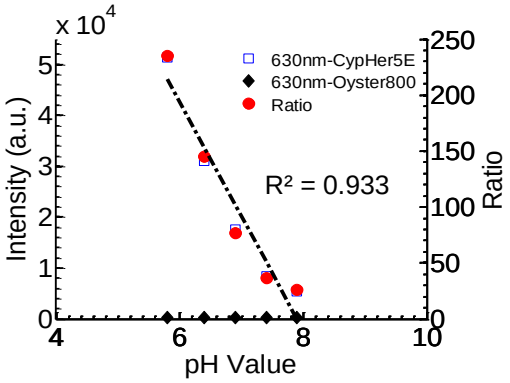

(b)

Figure 4-3 Ratiometric Fluorescence: (a) Kodak Two Wavelengths Excitation (b) Kodak Single Wavelength Excitation

This calibration is tested under system III and Kodak *In Vivo* FX Pro. The signal by detecting five samples of different pH value, 5.8, 6.4, 6.9, 7.4, and 7.9, labelled with two fluorescence dyes can form a linear relation as shown in figure 4-2 and figure 4-3. The blue squares represent 625nm light exciting CypHer5E whereas black diamond represents 625nm or 735nm light exciting Oyster800. After taking the ratio between blue squares and black diamond, the result is plotted as red circles. By analyzing the linear fitting of yellow triangle which is the ratio of two dyes, it can bring about the result of linear relation. In two wavelength excitation, either spot LEDs system or Kodak *In Vivo*

FX Pro, the linear correlation revealed by R^2 whereas similar in single wavelength excitation. From this data, it shows single wavelength excitation is capable on *in vivo* imaging detection by using ratiometric fluorescence pH probe.

Low Concentration Detection *in Vitro*

Fluorescence and bioluminescence imaging system should be capable on low concentration detection. Particularly for single wavelength excitation, since 625nm is far away from the absorption peak of Oyster800 which means very low quantum efficiency, the system performance decides the feasibility of it. If the emission light under low concentration related to low quantum efficiency can still receive the signal and get the similar permanence as 735nm exciting Oyster800 which reveals the fact that the system is capable on sensitivity.

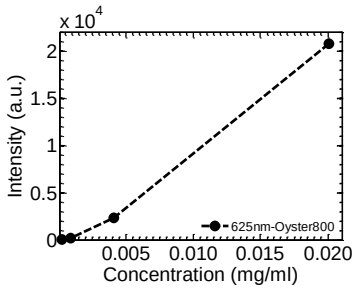

(a)

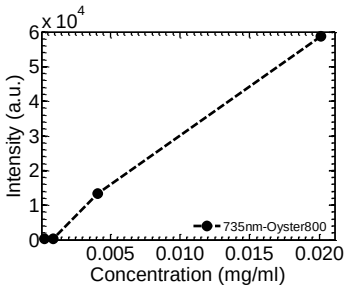

(b)

Figure 4-4 Low Concentration Calibration of Single Wavelength Excitation: (a) 625nm Exciting Oyster800 (b) 735nm Exciting Oyster800

For sensitivity, we tested four different concentrations of Oyster800 under two kinds of excitation light. The concentrations include 0.02 mg/ml, 0.004 mg/ml, 0.0008 mg/ml, and 0.00016mg/ml. From figures, the linear relation is similar but the relative intensity value of 625nm excitation is much lower than 735nm excitation. It's qualified the theoretical analysis and proven the feasibility of low concentration detection even with low quantum efficiency.

Chapter 5

Real System Performance

From two spot LEDs as a light source to single LED ring, the system is optimized to have a better performance. LED ring makes the system more compact without damage to the system performance, and the whole system can be electronically controlled except the filter wheel which has a manually controllable section outside the box. In this section, we bring a commercial product Kodak *In Vivo* FX Pro to join the comparison. By comparing three systems, single wavelength excitation, two wavelengths excitation, and Kodak, we can find the feasibility of our design.

For *in vitro* calibrations, besides light uniformity, all measurements are using small tubes filled with fluorescence pH probe on different pH value or concentrations. We used the same samples and set the same light intensity and exposure time. Without changing any conditions, samples have been run in three devices.

Light Uniformity

Light uniformity plays a vital role in imaging systems. If the light is not uniform, different positions may cause the incident intensity difference. It related to the output signals that can be detected. Hence, the un-uniform light brings a huge error as a result. We tested three kinds of LEDs: 625nm spot LED, 630nm LED ring, and white light 175W Xenon in Kodak. By using white paper as a test medium, it can reveal the exact light beams when they arrive at samples.

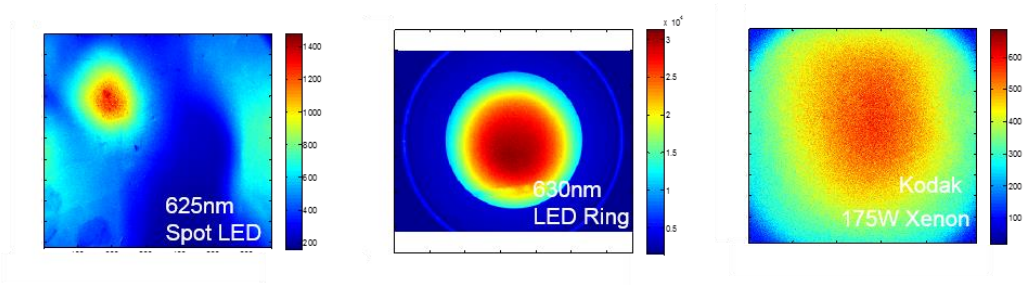

(a)

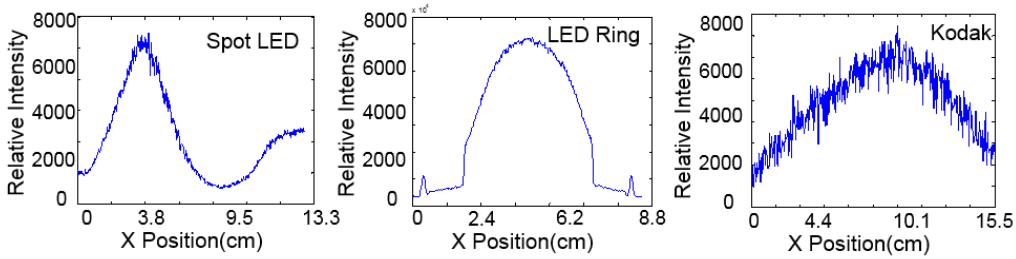

(b)

Figure 5-1 Light Uniformity: (a) Three Kinds of Uniformity of Light Output (b) The Cross Section of These Different Light Sources

From figures 5-1(b), the cross section reveals the uniformity of the beam clearly. For spot LED with 625nm wavelength, the incident angle and bad position make the beam form a small point which not only limits the effective area but also reduces the uniformity. For LED ring, it can form a perfect area with uniform beam. By calibrating the effective area, it will achieve 3cm*3cm reducing 20% intensity from peak value. Moreover, for Kodak, besides the oscillation of the beam intensity, the uniformity is the best of the three. But due to the oscillation, it may bring about some noise in the detection. Therefore, the spot LED has been suspended due to bad uniformity.

pH Ratiometric Analysis *in Vitro*

After adopting LED ring to rebuild the system, the comparison between Kodak and BLI can reveal the feasibility of setup. Utilizing four tubes with different pH value

labelled with two kinds of dyes (pH-sensitive CypHer5E and pH-insensitive Oyster800), we can calculate the ratio of these two dyes in order to get the perfect linear relation. Comparing BLI system (with LED ring) with Kodak, we can find the difference to commercial product. By plotting the data into figure 5.2, the linear fitting value R^2 reveals the level of linear relation.

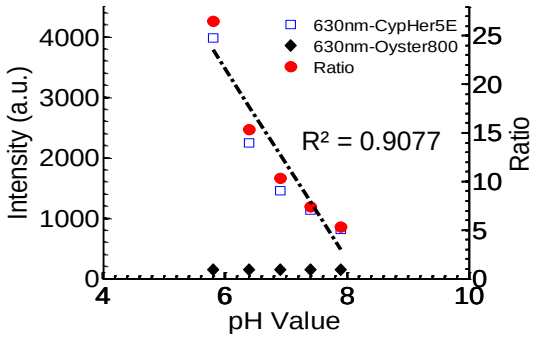

Figure 5-2 Single Wavelength Ratiometric Fluorescence of LED Ring Design

In the figures, blue squares represent the emission from CypHer5E whereas the black diamond represents emission from Oyster800. The red circles represent the ratio of these two dyes. Comparing with previous results of spot LED design and the Kodak system, it's obvious to find the similar linear correlation revealed by the ratio of two fluorescence dyes. Although emission intensity that photons collected by our device is much lower than Kodak, they can perform similar linear correlation corresponding on different pH values.

Low Concentration Detection *in Vitro*

We tested the BLI (with LED ring) system and compared it with Kodak for low concentration calibration. The test sample includes 0.00625 mg/ml, 0.003125 mg/ml, 0.0015625 mg/ml, 0.000390625 mg/ml, and 0.000195313 mg/ml. Each tube has two dyes labelled on the biosensor: Oyster680 and Oyster800. Low concentration means less biosensors in the solution which bring about low quantum efficiency. It is a test for the

system regarding its sensitivity. Even if the quantum efficiency is very low, *in vivo* imaging system is able to take the image of signals and proof of the feasibility that device can be used in pre-clinical research since the light emitted from human or animal body is very subtle.

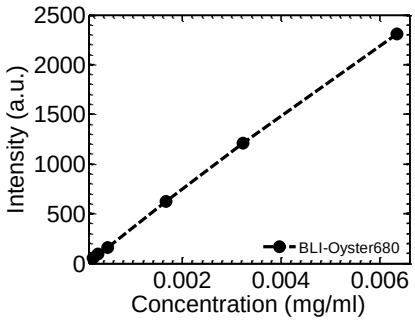

(a)

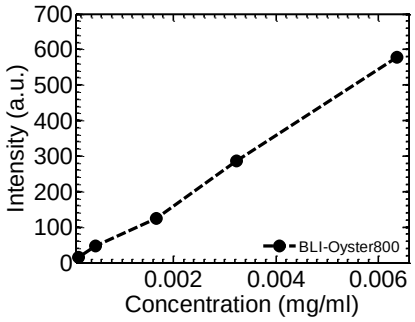

(b)

Figure 5-3 Low Concentration Calibration: (a) 630nm LED Ring Exciting Oyster680 in BLI System (b) 630nm LED Ring Exciting Oyster800 in BLI System

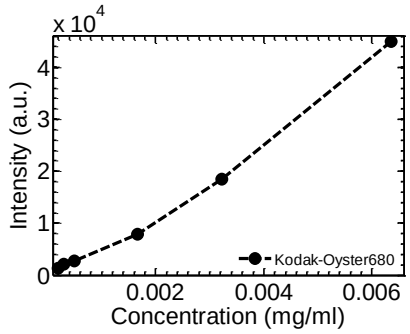

(a)

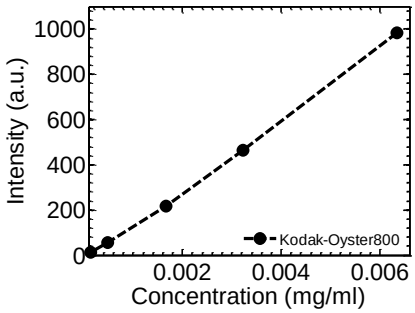

(b)

Figure 5-4 Low Concentration Calibration: (a) 630nm Exciting Oyster680 in Kodak System (b) 630nm Exciting Oyster800 in Kodak System

From the chart, it reveals the performance of two systems which are similar. Since the concentration of samples decrease 5 times, the relative intensity that has been detected should present a linear relation. Due to the effect of background noise and the characteristic of the biosensor, which is hard to keep at the same quantum efficiency, the linear relation is only roughly present. In figures, it is obvious to find a clear linear relation between different samples which prove the feasibility of the BLI system for *in vivo* imaging detection. The much lower relative intensity also points out a flaw of the BLI system and its low quantum efficiency.

Low Concentration Detection *in Vivo*

Since the low concentration detection *in vitro* shows the flaw of low quantum efficiency for the BLI system, it is necessary to process *in vivo* calibration which will reveal whether this low quantum efficiency qualifies the requirement of *in vivo* imaging. The purpose of the BIL system aims at helping to provide a noninvasive, rapid, and highly sensitive optical readout *in vivo*. It's necessary to see the performance of the system *in vivo*. We chose mouse as the dye carrier and injected different concentrations of Oyster680 & Oyster800: 0.1mg/ml, 0.02mg/ml, 0.004mg/ml. and 0.0008mg/ml.

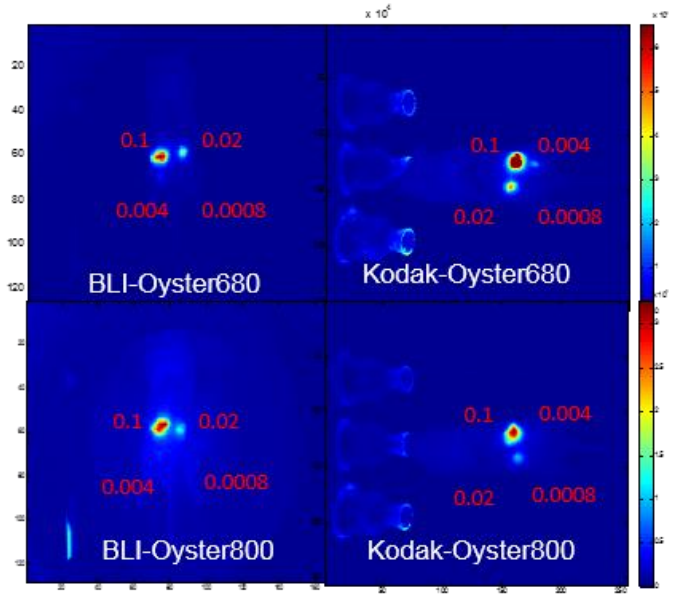

Figure 5-5 *In vivo* Fluorescent Imaging of Concentration Calibration for Mouse

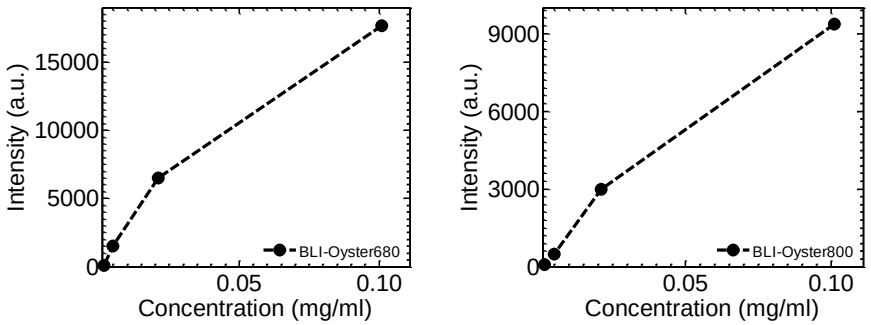

(a)

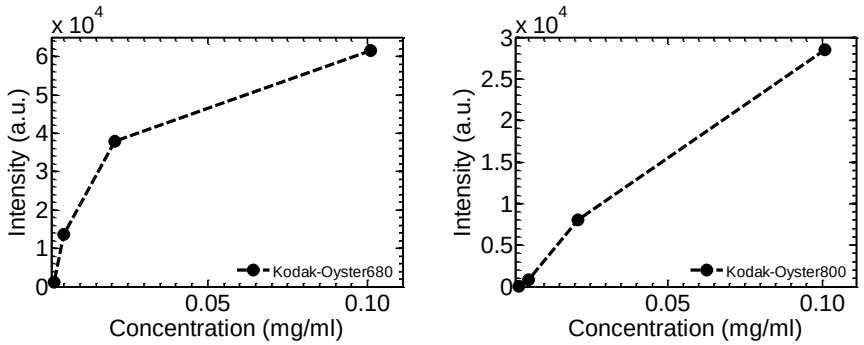

(b)

Figure 5-6 (a) Left: 630nm Exciting Oyster680 in LED Ring Design. Right: 630nm Exciting Oyster800 in LED Ring Design. (b) Left: 630nm Exciting Oyster680 in Kodak *In Vivo* FX Pro (saturated). Right: 630nm Exciting Oyster800 in Kodak *In Vivo* FX Pro.

From the figure, it is obvious to find that the performance of two systems are similar. However, it shows a saturated signal of high concentration sample in Kodak system exciting Oyster680. The sensitivity to collect emission photons in the Kodak system is better than our device. This may be caused by the capability of the camera and its field of view. Regardless of which one is used, our device shows the same analytical ability as Kodak.

Bioluminescence

Instead of fluorescence excited by incident light, luminescence is excited by chemical reactions, electrical energy, subatomic motions, or stress on a crystal. According to this, bioluminescence (L012) is excited by biological energy. Indeed, without external excitation source, the greatest performance of bioluminescence depends on the capability of the camera. The sensitivity of the camera should be high enough to capture the subtle signals.

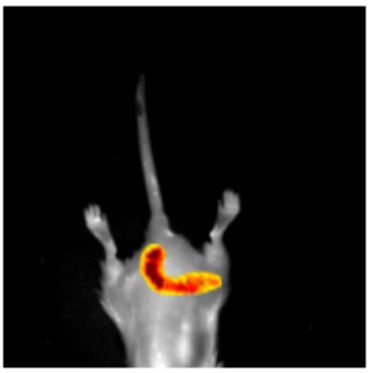

(a)

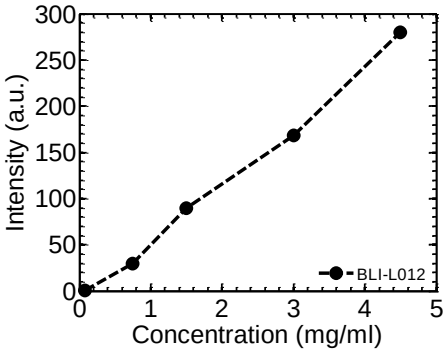

(b)

Figure 5-7 (a) Bioluminescence Imaging by BLI System (b) *In vivo* Bioluminescence of L012

In figure 5-7 (a), it shows the image of bioluminescence overlapping the image taken in the white light. By varying the concentration of L012 dye which contributes on bioluminescence, we can result in a linear correlation in figure 5-7 (b). From the result, it's persuasive to claim the BLI system of capable on bioluminescence detection.

Follow-up Calibration

LED ring has a divergence angle which brings about the uniformity changes accompanying distance. It's necessary to calibrate the optimal working distance. We defined the working distance as the length from the sample surface to the device bottom which can be quantitatively controlled in the future.

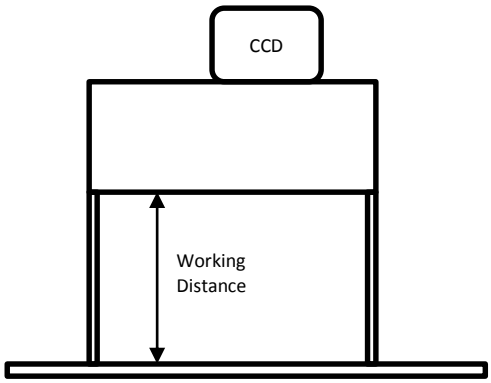

Figure 5-8 Definition of Working Distance

The working distance of LED ring on the datasheet is 4cm. After we calibrated (figure 5-8), 4~5cm can result in the best uniform light. The field of view is 8.8 cm (W) x 8.8 cm (L). And the beam size as defined above 80% of peak value part is 2.8 cm (W) x 3.5 cm (L).

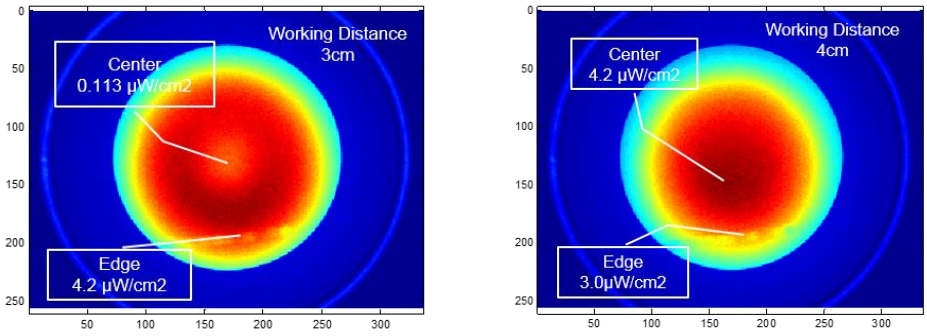

(a)

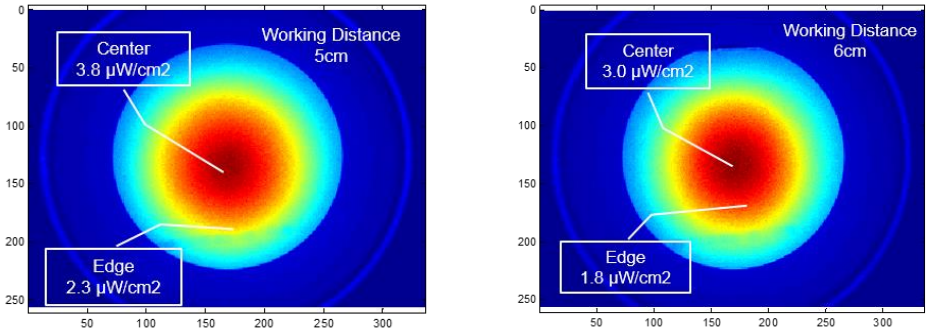

(b)

Figure 5-9 Calibration of Working Distance: (a) Left: 3cm. Right: 4cm. (b) Left: 5cm. Right: 6cm.

For working distance 3cm, the intensity of light at the center is much weaker than at the edge which means the light from each LED doesn't overlap. But for 4cm, 5cm and 6cm, the intensity of light at the center is a little stronger than at the edge, with a decreasing amount accompanying with distance. Therefore, the optimal working distance is 4cm.

Chapter 6

Conclusion

Compact and portable BLI system provides an extra view with most compact and portable dimensions when it comes to in-vivo measurement. The need to integrate optical modules into portable devices is increasing by the day. In order to achieve this, we need an optimized design that can help minimize the system dimension while still making system viable and inexpensive. In this paper we discuss how BLI system can be used to research in-vivo. By comparing with commercial product Kodak In-vivo FX Pro, it proves the feasibility of BLI. The various properties of BLI system such as high sensitivity and controllable incident intensity have been discussed in this paper. We also verified the feasibility of single wavelength (630nm) exciting two different dyes which is the most efficient way to make the system compact. Based on the calibration result of the final BIL system, it is competent for research.

Table 6-1 Specifications of BLI System

Specification	Value
Working Distance	4~5 cm
Incident Intensity	0~1000 μW/cm²
Exposure Time	0.010 ms – 70 min
Beam Size(@working distance 4cm)	2.8 cm(W) x 3.5 cm(L)
Imaging Area(@working distance 4cm)	8.8 cm(W) x 8.8 cm(L)
Device Dimension	7.5 cm(H) x 18.6 cm(W) x 21.1 cm(D)

Appendix A

Description of Components

Part	Vendor	PN	Specifications
LED Ring	Edmund Optics	#63-304	CL630nm FWHM30nm 100nm spot size at 40mm working distance 80W/m^2 irradiance at 40mm 100,000hr LED lifetime 70.8mm diameter 18mm height
CCD Camera	Hamamatsu	ORCA-R2	ER-150 Progressive scan interlined CCD 1344 x 1024 Effective Number of Pixels 6.45µm Pixel Size Effective area 8.67mm (H)×6.60mm (V) 10 µs to 4200 s Exposure time 0.0005 electrons/pixel/s (at -40 ℃) Dark Current 2×2, 4×4, 8×8 Binning –35°C forced air cooled –40°C water cooled(water temperature +20°C)
Lens	Thorlabs	MVL5M23	5 mm EFL f/2.8, for 2/3" Format Cameras, with Lock Field of View Field of View: 82.4° × 66.9°(2/3”); 65.2° × 51.3°(1/2”); 51.3° × 39.6°(1/3”)
700nm Filter	Edmund Optics	#67-905	CL700nm FWHM 10nm 50mm mounted diameter 5.9mm mount thickness >55% minimum transmission 200-10000nm blocking wavelength range ≥4.0 Optical Density OD
810nm Filter	Edmund Optics	#67-916	CL810nm FWHM 10nm 50mm mounted diameter 5.9mm mount thickness >50% minimum transmission 200-10000nm blocking wavelength range ≥4.0 Optical Density OD.

Appendix B

Matlab Imaging Processing Code

```
cd('C:\ ')   %folder path (where you put the data)
DIRNAME_PH = dir('name*parts*.tif');       % Find all filename (emission filter with 700) under the selected folder (remember: need to include the Binning4 in the front, and F700  in the middle)
DIRNAME_O800 = dir(' name*parts*.tif');     % Find all filename (emission filter with 810) under the selected folder (remember: need to include the Binning4 in the front, and F700  in the middle)


%%%%%%%%%%%%%%%%%%%%%%%%%%%%%%%%%%%%%%%%%%%%%%%%%%%%%%%%%%%%%%
% Select the area for sample and background (use the first image)

figure(1)
I = imread(char(DIRNAME_PH(1).name));      %Display the first image
imshow(mat2gray(I)); title('Please select the sample area')
ROI_SAMPLE = roipoly;      %select the area of sample (rough position of all samples)
title('Please select the background area')
ROI_BG = roipoly;   %select the area of background (area without any noise)
pause(0.2)

% using threshold method to select sample area (auto)
II = double(I).*double(ROI_SAMPLE);
ROI_SAMPLE_FINAL = im2bw(mat2gray(II));

%Display the result to make sure the area is correct
subplot(211);imshow(ROI_SAMPLE_FINAL)
subplot(212);imshow(ROI_BG)

%%%%%%%%%%%%%%%%%%%%%%%%%%%%%%%%%%%%%%%%%%%%%%%%%%%%%%%%%%%%%%
% Porocess all data set from the folder
for i = 1:length(DIRNAME_PH)
   I_PH = imread(char(DIRNAME_PH(i).name));   % Read the PH image from the folder
   I_O800 = imread(char(DIRNAME_O800(i).name));   % Read the O800 (pH independent) image from the folder

   % Display images with select area
   figure(2)
   subplot(211);imshow(mat2gray(double(I_PH).*double(ROI_SAMPLE_FINAL)))  %sample
   subplot(212);imshow(mat2gray(double(I_PH).*double(ROI_BG)))           % background

   % You can read the pH or Concentration information if you include your
   % value in your filename, remember to set the specific character
   %str  = DIRNAME_PH(i).name;
   %pH_Value(i) = str2num(str(length(str)-6:length(str)-4));

   % Calculate the average value for pH sample
   Data_PH(i,1) = mean(I_PH(find(ROI_SAMPLE_FINAL==1)));   % sample area
   Data_PH(i,2) = mean(I_PH(find(ROI_BG==1)));            % BG area
```

```
    Data_PH(i,3) =  Data_PH(i,1) - Data_PH(i,2);            % sample -BG

    % Calculate the average value for O800 sample
    Data_O800(i,1) = mean(I_O800(find(ROI_SAMPLE_FINAL==1))); % sample area
    Data_O800(i,2) = mean(I_O800(find(ROI_BG==1)));           % BG area
    Data_O800(i,3) =  Data_O800(i,1) - Data_O800(i,2);        % sample -BG

    % Calculate the ratio value for pH and O800 sample
    DATA_RATIO(i) = Data_PH(i,3) /Data_O800(i,3);

    pause(0.2)
end

 % You can plot the data if you read the information from filename
          % plot(pH_Value,DATA_RATIO,'o')
```

References

[1] Weissleder R, Mahmood U. Molecular imaging. Radiology. 2001 May;219(2):316-33.

[2] Barbet J, Peltier P, Bardet S, et al. Radioimmunodetection of medullary thyroid carcinoma using indium-111 bivalent hapten and anti-CEA x anti-DTPA-indium bispecific antibody. J Nucl Med 1998; 39:1172–1178.

[3] Hu S, Shively L, Raubitschek A, et al. Minibody: a novel engineered anti-carcinoembryonic antigen antibody fragment (single-chain Fv-CH3) which exhibits rapid, high-level targeting of xenografts. Cancer Res 1996; 56:3055–3061.

[4] Goodwin DA, Meares CF, Osen M. Biological properties of biotin-chelate conjugates for pretargeted diagnosis and therapy with the avidin/biotin system. J Nucl Med 1998; 39:1813–1818.

[5] Tjuvajev JG, Finn R, Watanabe K, et al. Noninvasive imaging of herpes virus thymidine kinase gene transfer and expression: a potential method for monitoring clinical gene therapy. Cancer Res 1996; 56:4087–4095.

[6] Gambhir SS, Barrio JR, Phelps ME, et al. Imaging adenoviral-directed reporter gene expression in living animals with positron emission tomography. Proc Natl Acad Sci USA 1999; 96:2333–2338.

[7] Weissleder R, Tung CH, Mahmood U, Bogdanov A Jr. In vivo imaging of tumors with protease-activated near-infrared fluorescent probes. Nat Biotechnol 1999; 17:375–378.

[8] Lyons SK. Advances in imaging mouse tumour models in vivo. J Pathol. 2005 Jan;205(2):194-205.

[9] Luker GD, Luker KE. Optical imaging: current applications and future directions. J Nucl Med. 2008 Jan;49(1):1-4. Epub 2007 Dec 12.

[10] Pomper MG. Translational molecular imaging for cancer. Cancer Imaging. 2005 Nov 23;5 Spec No A:S16-26.

[11] van der Meel R, Gallagher WM, Oliveira S, O'Connor AE, Schiffelers RM, Byrne AT. Recent advances in molecular imaging biomarkers in cancer: application of bench to bedside technologies. Drug Discov Today. 2010 Feb;15(3-4):102-14. doi: 10.1016/j.drudis.2009.12.003. Epub 2009 Dec 24.

[12] Hickson J. In vivo optical imaging: preclinical applications and considerations. Urol Oncol. 2009 May-Jun;27(3):295-7. doi: 10.1016/j.urolonc.2008.10.030.

[13] Coatney RW. Ultrasound imaging: principles and applications in rodent research. ILAR J. 2001;42(3):233-47.

[14] Deroose CM1, De A, Loening AM, Chow PL, Ray P, Chatziioannou AF, Gambhir SS. Multimodality imaging of tumor xenografts and metastases in mice with combined small-animal PET, small-animal CT, and bioluminescence imaging. J Nucl Med. 2007 Feb;48(2):295-303.

[15] Grassi R1, Cavaliere C, Cozzolino S, Mansi L, Cirillo S, Tedeschi G, Franchi R, Russo P, Cornacchia S, Rotondo A. Small animal imaging facility: new perspectives for the radiologist. Radiol Med. 2009 Feb;114(1):152-67. doi: 10.1007/s11547-008-0352-8. Epub 2008 Dec 11.

[16] Robertson R1, Germanos MS, Li C, Mitchell GS, Cherry SR, Silva MD. Optical imaging of Cerenkov light generation from positron-emitting radiotracers. Phys Med Biol. 2009 Aug 21;54(16):N355-65. doi: 10.1088/0031-9155/54/16/N01. Epub 2009 Jul 27.

[17] Lyons SK. Advances in imaging mouse tumour models in vivo. J Pathol. 2005 Jan;205(2):194-205.

[18] Pautler RG. Mouse MRI: concepts and applications in physiology. Physiology (Bethesda). 2004 Aug;19:168-75.

[19] Tsai, Y.-T., Zhou, J., Weng, H., Shen, J., Tang, L. and Hu, W.-J. (2014), Real-Time Noninvasive Monitoring of In Vivo Inflammatory Responses using a pH Ratiometric Fluorescence Imaging Probe. Advanced Healthcare Materials, 3: 221–229. doi: 10.1002/adhm.201200365

[20] Jay Reichman. Handbook of optical filters for fluorescence microscopy. Chroma technology corp. June 1998.

[21] Alex Fong, Bob Bronson, and Elliot Wachman. Advanced photonic tools for hyperspectral imaging in the life sciences. 15 April 2008, SPIE Newsroom. DOI: 10.1117/2.1200803.1051

[22] Warren. J. Smith. Modern optical engineering. Fourth edition. DOI: 10.1036/0071476873

[23] Mathieu Verdurand, Vu Nguyen, Daniela Stark, David Zahra, Marie-Claude Gregoire, Ivan Greguric, and Katerina Zavitsanou. Comparison of Cannabinoid CB1 Receptor Binding in Adolescent and Adult Rats: A Positron Emission Tomography Study Using [^{18}F]MK-9470. International Journal of Molecular Imaging. Volume 2011 (2011), Article ID 548123, 11 pages

[24] Abdel Wahad Bidar , Karolina Ploj , et al. In vivo imaging of lipid storage and regression in diet-induced obesity during nutrition manipulation. American Journal of Physiology - Endocrinology and MetabolismPublished. 1 December 2012Vol. 303no. E1287-E1295DOI: 10.1152/ajpendo.00274.2012

[25] Israt S. Alam1, Andre Neves1, et al. Fluorescence imaging of tumor cell death using C2Am. University of Cambridge, Cambridge, United Kingdom

Biographical Information

In 2011, Zhaoqiang Peng graduated from Shenzhen University in China with a Bachelor Degree in Electro-optic Information Engineering. During his undergraduate study, he finished several projects related to optics: Design of X-Ray Compound Refractive Lenses, Manufacture of Linear Light Source, Development of LED Coaxial Lighting Source, and Development of LED Backlighting Source. The charm of optical system is the constant impetus for his painstaking efforts. After that, he went to SANMINA-SCI Co., Ltd. (Shenzhen) to be a Quality Assurance Engineer mainly focusing on product false analysis and assembly line supervision which related to optical communication.

In 2012, he came to University of Texas at Arlington to pursue an Electrical Engineering Master's Degree with a focus on Bioluminescence & Fluorescence Imaging System. Out of keen interest, he has been growing up continually, from basic theory to the senior and from basic experiment to project research. The preciseness and patience is key work for him to complete his master's degree.

In the future, he is considering being an engineer in the industrial field or pursuing a PhD degree. Regardless, his choice always follows the interests of optics.